JOURNAL OF MATERIALS SCIENCE 24 (1989) 3387–3398

Mechanisms for rate effects on interlaminar fracture toughness of carbon/epoxy and carbon/PEEK composites

K. FRIEDRICH, R. WALTER
Polymer and Composites Group, Technical University Hamburg-Harburg, 2100 Hamburg 90, West Germany

L. A. CARLSSON
Department of Mechanical Engineering, Florida Atlantic University, Boca Raton, Florida 33431, USA

A. J. SMILEY
ICI Composites Structures, 2055 East Technology Circle, Tempe, Arizona 85284, USA

J. W. GILLESPIE Jr
Center for Composite Materials, University of Delaware, Newark, Delaware 19716, USA

The objective of this study was to investigate strain-rate dependent energy absorption mechanisms during interlaminar fracture of thermosetting (epoxy) and thermoplastic (PEEK) unidirectional carbon fibre (CF) composites. A simple model addressing the translation of matrix toughness to mode I and mode II interlaminar toughness of the composite is presented, in conjunction with a fractographic examination of the fracture surfaces and the fracture process. The observed rate dependency of composite fracture toughness is attributed to the rate-dependent toughness of the viscoelastic matrix and the size of the process zone around the crack tip. Other important factors identified are the roughness of the fracture surface and fibre bridging.

1. Introduction

The interlaminar mode of fracture of laminated composites has aroused considerable attention from a durability and damage tolerance viewpoint. This failure mode is of special concern because delaminations are not visible and they can lead to substantial reductions in stiffness and strength of a structure. Delamination can be introduced during manufacturing as a result of contamination of the prepreg. More serious perhaps is foreign body impact that may cause multiple delaminations in the structure. Repeated loading can lead to the propagation of these cracks and subsequent failure of the composite structure [1]. The resistance of the material to interlaminar crack growth is commonly quantified by the interlaminar fracture energy, G_c, also designated as interlaminar fracture toughness. Because an interlaminar crack propagates in the resin-rich region between plies, the energy absorption during interlaminar fracture is mainly related to the work of deformation of the polymer matrix [2]. Brittle matrix composites are generally tougher than the bulk matrix. The reverse is true for ductile matrix composites where the rigid elastic fibres restrict the size of the plastic zone that develops at the crack tip between plies [2]. In unidirectional composites, peeling and failure of fibres bridging the crack surfaces can also contribute to the fracture energy [3, 4]. In addition, the bond quality of the fiber/matrix interface influences the delamination fracture energy [5].

It should be recognized that polymeric matrices are viscoelastic materials. Fracture studies of unreinforced polymers have consequently shown that the resistance to plastic deformation (yield stress), the strain to failure and the fracture toughness, are strongly-dependent on temperature and strain rate [6–9]. It has also been shown that the composite interlaminar fracture energy, G_c, is sensitive to strain rate. Previous investigations by Smiley and Pipes [10–12] show that severe reductions in the mode I and mode II toughness of carbon fibre (CF)/epoxy and CF/PEEK composites occur at high strain rates. Scanning electron microscope (SEM) studies of the fracture surfaces were performed to investigate mechanisms associated with the reduction in toughness [10–12]. The CF/PEEK fracture surfaces displayed a larger extent of plastic deformation at low rates than at high rates consistent with the reduction of fracture toughness at high rates. The CF/epoxy fracture surfaces did not display any noticeable change

0022–2461/89 $03.00 + .12 © *1989 Chapman and Hall Ltd.*

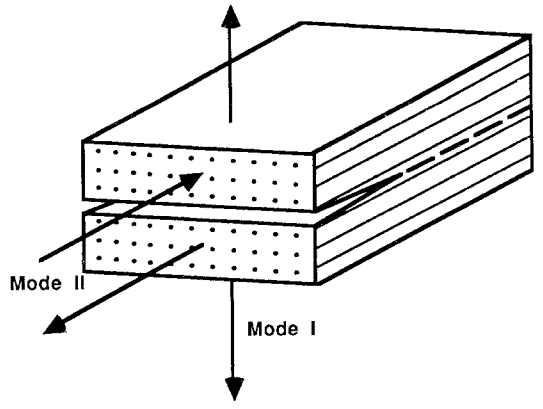

Figure 1 Illustration of the opening (mode I) and forward shearing (mode II) modes of crack surface displacements.

in microscopic deformation behaviour that would explain the rate sensitivity [11, 12].

To investigate further the rate-dependent fracture mechanisms and the translation of matrix toughness to the composite interlaminar fracture toughness, *in situ* SEM studies were performed in modes I and II and the test specimens previously fractured [11, 12] were examined in greater detail in the SEM.

2. Materials and methods

In this section the results from the previous studies [11, 12] on rate effects of mode I and II fracture toughness are briefly reviewed.

2.1. Materials

The carbon/epoxy composite is the AS4/3501-6 system produced by Hercules. The prepeg material was processed in a autoclave using the supplier-recommended cure cycle to obtain a fibre volume fraction of 66% [11, 12]. The carbon/PEEK utilized is the APC-2 material produced by Imperial Chemical Industries. The carbon fibre (AS4) volume fraction of the APC-2 was 62%. PEEK is a thermoplastic semi-crystalline polymer and requires a relatively high processing temperature (380° C) and a rapid cooling rate ($> 10°\,C\,min^{-1}$) to achieve the appropriate morphology of the matrix (about 30% crystallinity). This was achieved in a compression press fitted with internally cooled platens [11, 12].

2.2. Fracture tests

Fracture testing of the materials was performed at a large range of cross-head speeds under the opening (mode I) and forward shearing (mode II) modes of fracture illustrated in Fig. 1. For mode I testing, straight-sided $[0]_{26}$ double cantilever beam (DCB) specimens were used [13]. For the mode II tests, $[0]_{24}$ and $[0]_{26}$ end-notch flexure (ENF) specimens were employed [13]. The geometries of the specimens used and a description of data reduction of the interlaminar fracture toughnesses, G_{Ic} and G_{IIc}, are described in previous papers [10–12]. Under quasi-static fixed grip loading, stable crack growth is predicted in the DCB test while unstable growth is predicted for the ENF test [13]. For viscoelastic matrices like PEEK, however, the stability of crack growth is dependent upon the strain rate. For example, unstable crack growth in the DCB and stable crack growth in the ENF tests

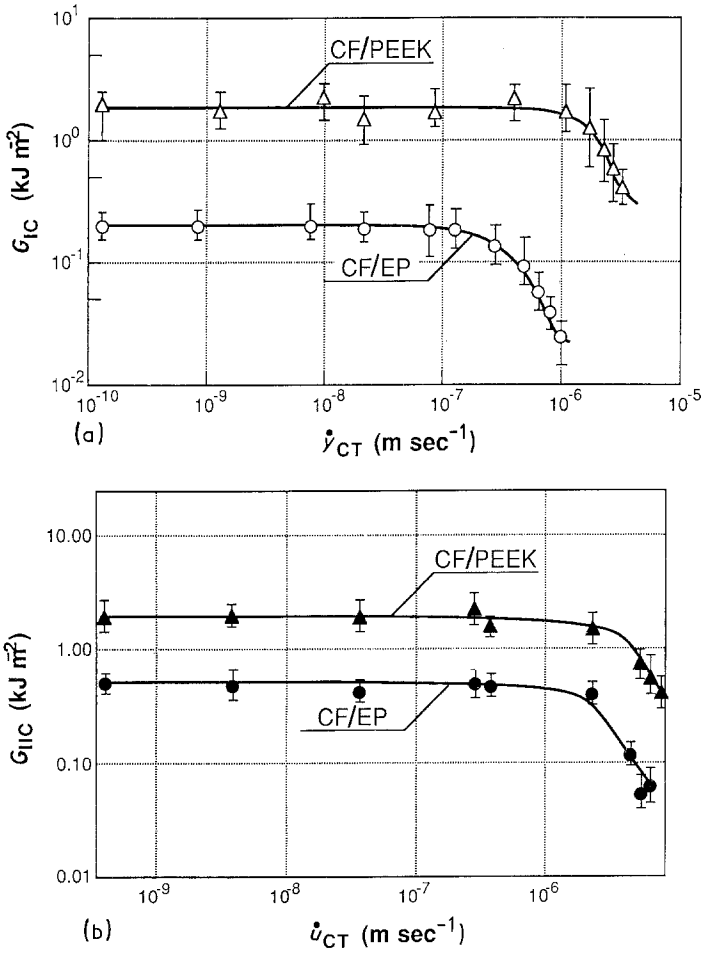

Figure 2 Fracture energy plotted against crack tip displacement rate in CF/PEEK and CF/epoxy [10–12]: (a) log–log scale for mode I; (b) log–log scale for mode II.

have been observed in the CF/PEEK system, depending on the cross-head speed [11, 12, 14, 15]. This will be discussed in subsequent sections.

The fracture toughness was evaluated previously from the initial compliance and the maximum load [11, 12]. Consequently, the toughness reported [11, 12] refers to initiation of fast fracture. To relate the fracture toughness to the local behaviour at the crack tip, crack tip displacement rates for mode I and mode II, $\dot{y}_{CT}$, and $\dot{u}_{CT}$, respectively, were determined as a function of cross-head speed ($\dot{\delta}$) and geometry parameters [11, 15]

$$\text{Mode I} \qquad \dot{y}_{CT} = 1.5\dot{\delta}\xi^2 \tag{1}$$

$$\text{Mode II} \qquad \dot{u}_{CT} = \frac{24\dot{\delta}ha^2\xi}{(2L^3 + 3a^3)} \tag{2}$$

ξ is a nondimensional distance from the crack tip, $\xi = x/a$, where $x = 0.25$ mm and a is the crack length. h and L are semi-thickness and semi-span, respectively, of the ENF geometry.

The results of these studies are summarized in Fig. 2. In the double logarithmic plots of G_{Ic} against $\dot{y}_{CT}$ and G_{IIc} against $\dot{u}_{CT}$, it is observed that over a large range of low and medium crack tip displacement rates there is no remarkable effect of rate on fracture energy. Above a critical rate, the mode I and II toughnesses of both composites drop rapidly to an apparent minimum level.

3. Fracture model

To provide further insight into the results shown in Fig. 2, i.e. the constant toughness at low and intermediate rates and the drop in toughness at high rates, the model illustrated in Fig. 3 is considered as a basis for the fractographic investigation subsequently presented. Fig. 3 is a schematic representation of the micromechanisms responsible for energy absorption during mode I and mode II loading. The following energy absorbing factors are considered: (i) formation of the fracture surface of the main crack; (ii) plastic deformation and/or microcracking of the matrix in the damage zone around the crack. The larger the damage zone, the more side cracks and bridged fibres are expected; (iii) crack bridging by fibres or fibre bundles, resulting in fibre peeling and fractures.

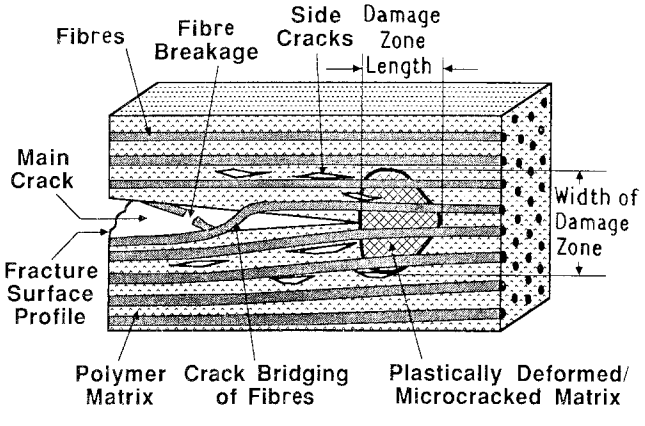

Figure 3 Schematic illustration of possible mechanisms of energy absorption during interlaminar fracture of unidirectional composites.

It is reasonable to assume that the interlaminar fracture toughness is related to the following quantities: the surface area of the new fracture surface; $G_{c,m}$ = fracture energy of the matrix; $(DZS)_c$ = volume of plastically deformed matrix in the damage zone formed at the crack tip in the composite; w_p = energy for peeling bridged fibres; n_p = number of debonded and bridged fibres per unit area; w_f = energy for fibre fracture; and n_f = number of fractured fibres per unit area of fracture surface. The interlaminar toughness is expected to increase with an increase in any of the above quantities.

The actual fracture surface area created during interlaminar failure may be significantly larger than the projected area (width × crack increment) used in the determination of G_c. The fracture surface may contain hackles and may not be planar as indicated in Fig. 3. To incorporate approximately the roughness of the fracture surface in a quantitative description of the toughness transfer from matrix to composite, fracture surface profiles as illustrated in Fig. 4 may be determined from examination of cross-sections of the fractured specimens. The surface roughness is quantified by the profile length, L_r, over the projected length, L_p. A similar quantity was introduced by Crick *et al.* [16].

The second factor considered important for the toughness transfer from matrix to composite is the volume of plastically deformed and microcracked polymer at the crack tip between plies in the composite $(DZS)_c$. This factor has been discussed and examined in some detail by Bradley and Cohen [5] and Hunston [2]. Based on the assumptions that the process zone for the composite has the same volume as the bulk polymer and the toughness of the composite is derived by energy dissipation in the polymer matrix, Bradley and Cohen [5] suggested the following formula for the composite interlaminar toughness

$$G_c \approx G_{c,m} v_m \tag{3}$$

where G_c and $G_{c,m}$ are the toughness of the composite and the bulk resin, respectively, and v_m is the average

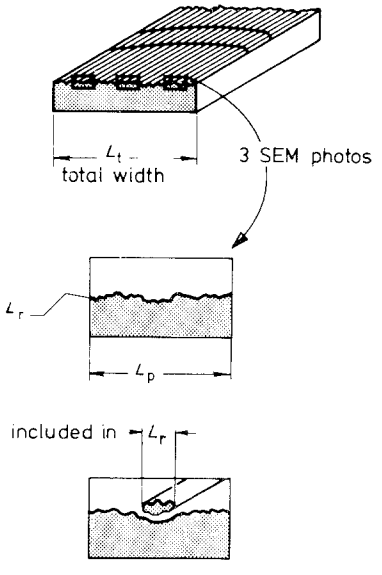

Figure 4 Schematic illustration of fracture surface profile determination.

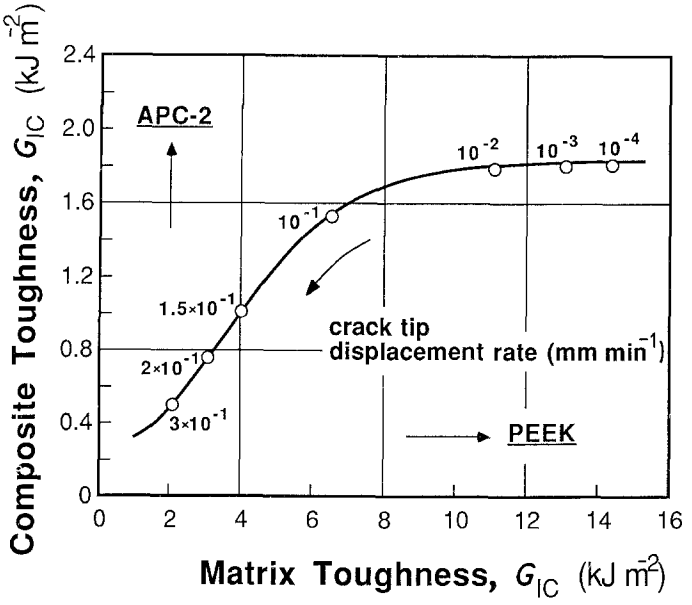

Figure 5 Relationship between the fracture energy of PEEK matrix and CF/PEEK composite with the crack tip displacement rate as parameter.

matrix volume fraction over the process zone. For delamination failure, v_m averages the resin-rich region between plies and the lower matrix fraction of the fibre layers. Consequently, v_m is less than unity and larger than 0.4 for the composites studied herein.

To include surface roughness and peeling and fracture of bridged fibres the following extension of Equation 3 is proposed

$$G_c \approx \frac{L_r}{L_p} v_m G_{c,m} + w_f n_f + w_p n_p \quad (4)$$

This equation incorporates the fracture surface profile and peeling and fracturing of debonded fibres. A similar expression for the interlaminar toughness of the composite was proposed by Crick *et al.* [16]. They did not, however, consider the restrictions imposed on the plastic zone at the crack tip between plies. Note that Equation 4 is expected to hold for both mode I and mode II loading. If G_c and $G_{c,m}$ are different in mode I and mode II the appropriate toughness have to be substituted into Equation 4. Also note that all parameters in Equation 4, except the specific energy for fibre fracture (w_f), are likely to be strain-rate dependent. It is expected that the first term in Equation 4, which involves the toughness of the matrix, dominates the contribution to the composite interlaminar toughness. The second and third terms might, however, be significant in situations where fibre bridging occurs. As shown by Russell and Street [3] and Johnson and Mangalgiri [4], fibre bridging requires unidirectional plies above and below the delamination plane and is predominant in mode I loading. But, as shown later in this paper, fibre bridging also may occur in mode II loading of unidirectional composites.

4. Results and discussion

The model presented here will be used as a basis for investigating rate effects on mode I and mode II interlaminar toughness. At this point is should be recognized that a quantitative comparison with Equation 4 is not possible because many of the parameters in this equation are unknown. For example, the mode II toughness values of the matrix materials investigated are unknown. Equation 4 will merely be used as a basis for discussion of information reduced from observations of the fracture behaviour and fracture surfaces and strain-rate dependency of the mechanical and fracture properties of the epoxy and PEEK materials considered. Factors investigated in this study are: relationship between matrix toughness and composite interlaminar fracture toughness, microscopic fracture studies through development of *in situ* SEM fixtures and analysis of fracture surface profiles. The extent of fibre bridging will be studied by counting broken fibres on the fracture surfaces.

TABLE I Mode I fracture toughness of bulk PEEK

$\dot{\delta}$ (mm min^{-1})	E (GPa)*	K_{Ic} (MPa m$^{1/2}$)	$G_{Ic} = \frac{K_{Ic}^2}{E}$ (kJ m^{-2})	$\dot{\gamma}_{CT}$ (mm min^{-1})†
10^{-1}	3.40	7.2	15.2	5.5×10^{-5}
10^{0}	3.60	6.6	12.1	5.5×10^{-4}
10^{1}	3.80	6.7	11.8	5.5×10^{-3}
10^{2}	4.00	6.4	10.2	5.5×10^{-2}
2×10^{2}	4.02	5.2	6.7	1.1×10^{-1}
3×10^{2}	4.05	4.0	3.9	1.6×10^{-1}
4×10^{2}	4.08	3.5	3.0	2.2×10^{-1}
5×10^{2}	4.10	3.0	2.2	2.8×10^{-1}
7×10^{2}	4.15	2.0	1.0	3.8×10^{-1}
10^{3}	4.20	1.2	0.3	5.5×10^{-1}

*Values estimated from manufacturer's data.
$^{\dagger}\dot{\gamma}_{CT} = 3\xi^2\dot{\delta}/(2a^2)$ with $\xi = 0.25$ mm and $a = 13$ mm.

4.1. Relationship between matrix toughness and interlaminar fracture energy

Several studies on the interlaminar fracture behaviour of continuous fibre–polymer matrix composites have shown that an increase in fracture toughness of the matrix results in an increase in the interlaminar fracture energy of the composite [2, 5, 16, 17]. Above a certain level of matrix toughness, however, a saturation in the composite toughness takes place because of the limited ability for expansion of the damage zone due to the presence of the rigid fibres [2, 5]. The relationship between matrix and composite toughness will be investigated here in terms of the observed rate dependency of matrix and composite fracture toughness under mode I loading.

Fracture toughness data of bulk PEEK were previously evaluated from compact tension specimens over a large range of cross-head speeds [19, 20]. Table I shows stress intensity (K_{Ic}) data transformed to G_{Ic} data at various cross-head speeds. Also shown is the crack tip opening rate, $\dot{y}_{CT}$, determined from Equation 1. It is observed that the toughness of the PEEK matrix continuously drops with increased strain rate. The matrix toughness drops substantially at crack tip opening velocities larger than 5.5×10^{-2} mm min^{-1}.

To relate the toughness of the matrix to the toughness of the composite, data at a given crack tip displacement rate were plotted as shown in Fig. 5. In the low velocity range (10^{-2} to 10^{-4} mm min^{-1}) the matrix toughness is greatest (10 to 14 kJ m^{-2}) and rate insensitive. Consequently, there is no change in interlaminar toughness of the CF/PEEK composite. As the crack tip velocity increases, the bulk PEEK toughness drops significantly and this is also observed in the composite. Alternatively, as strain rate decreases, an increase in toughness of the polymer matrix occurs that causes an increase in the interlaminar fracture toughness to a saturation level.

The mode I toughness of the PEEK matrix composite is always considerably less than the matrix toughness. For the extremely low rates the ratio of composite to matrix toughness is only about 0.13. This would indicate that the fibres in the composite constrain the plastic zone to a small volume and that the degree of constraint is most severe for PEEK at low rates. This is schematically illustrated in Fig. 6.

For the epoxy matrix composite the discussion of influence of rate on toughness is possible only in a more qualitative manner because data for the particular bulk resin are not available. Data from the literature [21, 22] do not characterize an identical epoxy system to the one use here (3501-6) Fig. 7 shows composite compared to matrix [21, 22] toughness over a large range of deformation rates. Similar to the situation in the PEEK matrix composition, the toughness of the epoxy matrix decreases when the toughness of the matrix decreases. For the brittle epoxy matix composite, the mode I toughness is less than that of the bulk matrix although the toughness is more effectively transferred than for the ductile PEEK matrix composite. Hunston [2] found, in contrast to the results presented here, that the toughness of brittle matrix composites may exceed the toughness of the neat resin. The difference is likely to be due to the fact that literature data [21, 22] for the bulk resin characterize a more ductile epoxy than the 3501-6 epoxy in the composite.

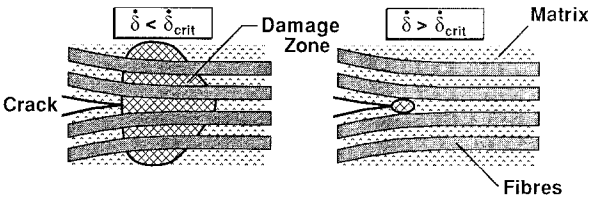

Figure 6 Schematic illustration of the damage zone at $\dot{\delta} < \dot{\delta}_{crit}$ and $\dot{\delta} > \dot{\delta}_{crit}$.

To investigate further restrictions on the plastic zone imposed by the fibres, the planar dimension of the plastic zone was calculated using Irwin's model [23]

$$r_p = \frac{K_{Ic}^2}{\pi \sigma_y^2} \quad (5)$$

where r_p is the plastic zone diameter for plane stress, K_{Ic} is the critical mode I stress intensity factor and σ_y is the yield stress of the material.

Table II gives plastic zone size (r_p) estimated for the two matrix materials as a function of crack tip velocity, and Fig. 8 shows the result in comparison to the scatter band of the fibre-to-fibre distances. Even at the highest velocity, the plastic zone is larger than the thickness of the matrix region between the plies. This supports the hypothesis that the damage zone around the crack tip spreads into the fibre layers. Consequently, the damage zone is highly restricted by the fibres in the composite and this qualitatively explains the less than one-to-one toughness transfer from matrix to composite.

From the discussion above it appears that the rate effects on mode I toughness can be rationalized by the rate dependency of the neat resin toughness. Unfortunately, due to lack of mode II toughness data of the

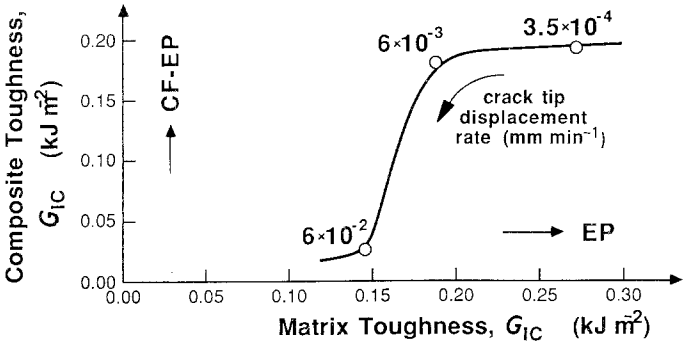

Figure 7 Composite toughness plotted against matrix toughness in mode I for epoxy with the crack tip velocity as parameter.

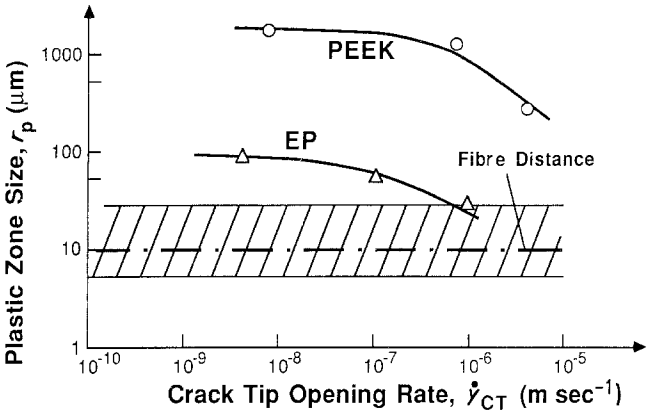

Figure 8 Plastic zone size, r_p, in epoxy and PEEK as a function of crack tip displacement rate, and in relation to the fibre-to-fibre distance in the composites (—·—) average distance.

resins this hypothesis cannot be examined in the mode II case. It is, however, expected that similar arguments would hold true also for the forward shearing mode.

4.2. *In situ* crack propagation studies

To study the damage zone and crack propagation mechanisms under different fracture modes, *in situ* fixtures illustrated in Fig. 9 were devised. This method was first applied to fracture studies of composites by Bradley and Cohen [5]. To achieve mode I propagation, a razor blade is pressed between the plies of a polished test specimen. For *in situ* crack propagation studies in mode II, a three-point bending fixture was devised, see Fig. 9. Although this study concerns interlaminar crack growth, the *in situ* studies were limited to intralaminar crack growth in unidirectional composites. The main difference is that the interlaminar crack growth occurs in an approximately 10 μm thick resin-rich region between plies (Fig. 8) while intralaminar cracks grow in a very thin resin region between fibres. For ductile resins this may provide quantitative differences in the toughness according to the discussion above. Qualitatively, the fracture mechanisms should be similar for both types of crack growth.

4.3. *In situ* mode I fracture

Fig. 10a shows the crack tip region around a mode I intralaminar crack in CF/PEEK that was opened slowly. The damage zone around the crack tip, as indicated by the dashed circle, extends over five to six fibre layers and over some distance ahead of the crack tip. The damage includes microcracks in the matrix, see Fig. 10b, microcracks between the matrix and the fibres in the interfacial region, plastically deformed matrix material and cracks adjacent to the main crack tip. The plastically deformed matrix between the fibres is easily observed in Fig. 11.

In the CF/epoxy system, *in situ* mode I cracks were studied at two different crack opening rates. A low rate was achieved by pressing the razor blade very slowly into the lamina. The result of this experiment is shown in Fig. 12. In CF/epoxy a damage zone is also observed around and ahead of the crack tip. The damage zone is, however, much smaller than in CF/PEEK. Two or three fibre layers around the main crack are involved in the fracture process that includes the formation of microcracks in the matrix between fibres and at the fibre/matrix interfaces. A very high magnification of the region ahead of the main crack tip, Fig. 12b, shows that failure of the epoxy matrix between the fibres takes place by microcrack formation.

A high crack tip displacement rate in the *in situ* experiment was created by impacting the razor blade into the CF/epoxy lamina. This resulted in a very rapid jump forward of only a single main crack with no side cracks. No characteristic damage zone could be identified around the tip of this crack. Even under very high magnification, Fig. 13, no microcracks are visible. Separation of the material takes place primarily along fibre/matrix interfaces.

These observations qualitatively support the simple calculations on the effect of strain rate on mode I plastic zone size presented in the previous section. The results also show that the damage zone extends into the resin around the fibres as illustrated schematically in Figs 3 and 6.

4.4. *In situ* mode II fracture

In situ mode II crack propagation was possible only at low crack tip displacement rates due to the simple device used in this study. Fig. 14 shows details of the damage mechanisms ahead of a mode II crack in CF/PEEK. Under the action of shear stress ahead of the crack tip, tensile cracks form in the matrix at 45°. In regions within the damage zone where the stress intensity is highest, i.e. very close to the crack tip,

TABLE II Rate dependency of damage zone size in bulk polymers

Material	K_{Ic} (MPa m$^{1/2}$)	σ_y (MPa)*	r_p (mm)†	$\dot{\gamma}_{CT}$ (m sec^{-1})
PEEK	6.6	100	1.38	9.1×10^{9}
	6.4	111	1.06	8.7×10^{-7}
	3.0	113	0.22	4.7×10^{-6}
EPOXY	0.98	60	0.084	5.2×10^{-9}
	0.81	65	0.050	1.0×10^{-7}
	0.72	69	0.034	1.0×10^{6}

*σ_y values estimated from the manufacturer's data.
†$r_p = K_{Ic}^2/(\pi\sigma_y^2)$ [23].

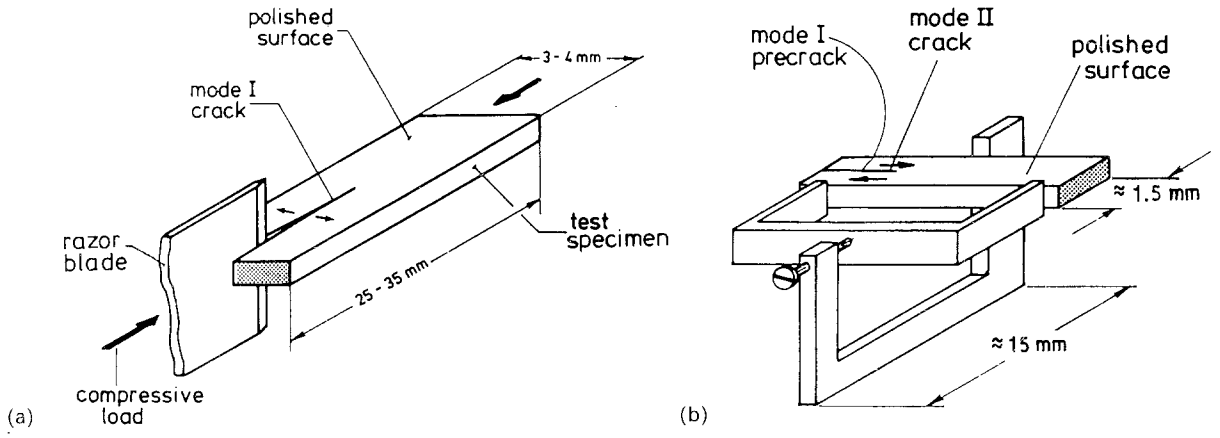

Figure 9 Fixtures for *in situ* crack propagation studies: (a) mode I, (b) mode II.

these cracks extend completely between neighbouring fibres. They then tend to propagate along the fibre–matrix interface and open up. Finally, separation of the matrix material between the cracks leads to the full development of the hackled mode II fracture surface. The damage zone in CF/PEEK under low velocity/mode II conditions is extended over four to six fibre layers.

Fig. 15 displays the mode II crack tip zone for CF/epoxy. At very high magnification it is observed that crack formation is similar to that observed in CF/PEEK. Because of the lower ductility of epoxy these cracks open up very easily and form the shear cusps shown in Fig. 15. In Fig. 15b a fibre bridging the two crack faces can be observed. Further extension of the crack would cause fracture of this fibre and a fibre breakage on the remaining fracture surfaces. A significantly smaller damage zone is observed in the more brittle CF/epoxy than in the ductile CF/PEEK which, according to the previous discussion, partly explains the observed difference in mode II toughness values between the two systems.

4.5. Fracture surface profiles

As discussed in conjunction with the model for energy absorption during interlaminar fracture, Fig. 3, the actual surface area of the newly created fracture surfaces may be significantly larger than the projected area used in the data reduction scheme for the determination of the interlaminar fracture energy, G_c.

The actual surface area of the new areas created may be estimated by evaluation of the fracture surface profile in a cross-section perpendicular to the crack direction. Fig. 4 is a schematic representation of the determination of the surface profiles which followed these steps:

(i) after polishing the edge, SEM photos were taken at three positions across the width;

(ii) the photos were magnified to allow measurement of the length, L_r, of the profile by the use of a graphic tablet;

(iii) if bundles of fibres were separated from the fracture surface the extra length which accounts for the additional fracture surface formed is included in L_r.

(iv) the L_r values achieved by this procedure were normalized with the projected length L_p, see Fig. 4.

Typical fracture surface profiles are shown in Fig. 16. Fig. 16a shows mode I profiles while mode II profiles are shown in Fig. 16b. To investigate whether the crack initiation region of a crack increment, where the toughness values shown in Fig. 2 were evaluated, possesses a different fracture surface profile than the region where the crack propagates in a stable or unstable manner, surface profiles were determined for both regions. A quantitative evaluation of these and similar photographs yields the data summarized in Table III. The data show that the fracture surface profile is about 20% to 50% greater than the projected length. This is certainly an important factor to consider in the translation of matrix toughness to composite toughness.

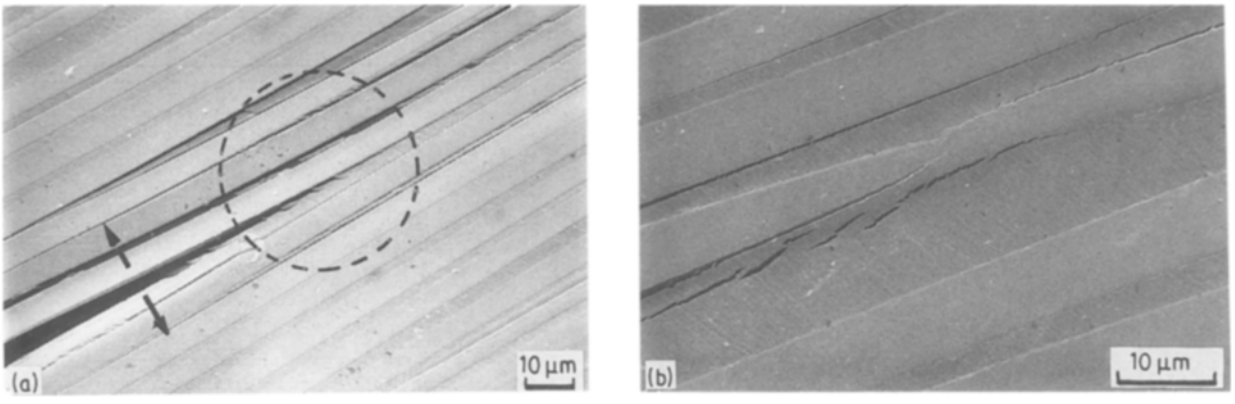

Figure 10 Slowly opened mode I crack (*in situ*) in CF/PEEK (dashed circle marks the approximate size of the damage zone around the crack tip).

TABLE III Fracture surface profiles

Material	Mode	Crack tip displacement rate ($m\,sec^{-1}$)	L_r/L_p	
			Initiation region	Propagation region
CF/PEEK	I	1×10^{-10}	1.66 ± 0.14	1.43 ± 0.04
CF/PEEK	I	4×10^{-6}	1.32 + 0.08 − 0.06	1.22 + 0.08 − 0.05
CF/epoxy	I	1×10^{-10}	1.24 + 0.01 − 0.02	1.29 + 0.05 − 0.04
CF/epoxy	I	1×10^{-6}	1.22 + 0.03 − 0.05	1.19 + 0.06 − 0.04
CF/PEEK	II	1×10^{-8}	1.23 ± 0.05	2.12 + 1.56 − 0.84
CF/PEEK	II	7×10^{-6}	1.29 + 0.01 − 0.02	2.07 + 0.42 − 0.53
CF/epoxy	II	1×10^{-8}	1.20 ± 0.04	1.36 + 0.06 − 0.12
CF/epoxy	II	5×10^{-6}	1.29 + 0.11 − 0.09	1.26 + 0.10 − 0.09

In the initiation region, the mode I fracture surface profiles of CF/PEEK are larger than the corresponding areas for CF/epoxy, while in mode II the surface areas are similar for both systems (Table III). With respect to rate effects on the surface profiles for the initiation region, CF/PEEK shows larger surface profiles in mode I at low rates than at high rates which partly explains the larger toughness observed at low rates. In mode II, however, no significant rate dependency is noted. The fracture surface profile of the epoxy system shows no significant rate dependency or dependency of the mode of loading. Based on these observations, the fracture surface profiles cannot explain the observed rate dependency of the fracture toughness.

Except for CF/PEEK fractured in mode II, the fracture surface profiles are similar in the initiation and propagation regions. The significance of the large fracture surface of CF/PEEK in the propagation region is, however, diminished by the large scatter, see Table III.

4.6. Fibre breakages

In studies on interlaminar fracture of unidirectional composites is has been shown that fracture of fibres that bridge the delamination may be a mechanism contributing to the interlaminar fracture energy [3, 4]. Sudden failure of bridging fibres has been proposed by Berglund [24] the mechanism responsible for the stick–slip fracture behaviour observed in mode I fracture of CF/PEEK composites.The stick-slip phenomenon is manifested by slow stable crack propagation interrupted by fast unstable growth. Gillespie *et al.* [14], on the other hand, explained the stick–slip behaviour in terms of two competing mechanisms that occur

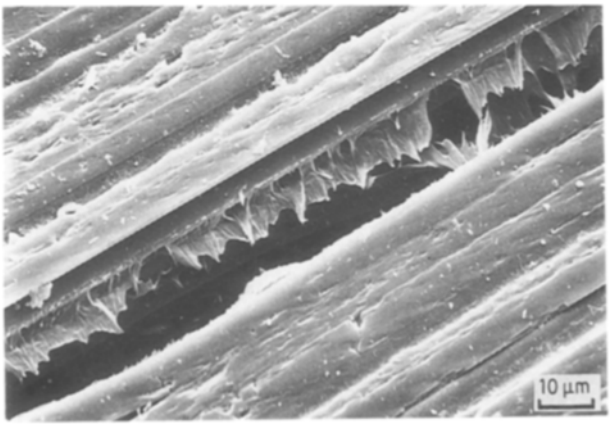

Figure 11 Very slowly opened mode I crack in CF/PEEK, giving evidence for significant deformation around the main crack.

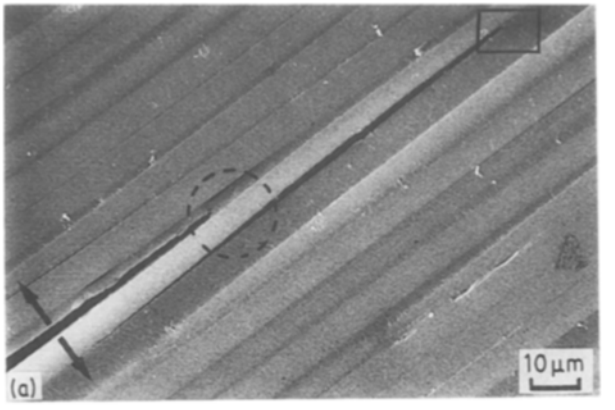

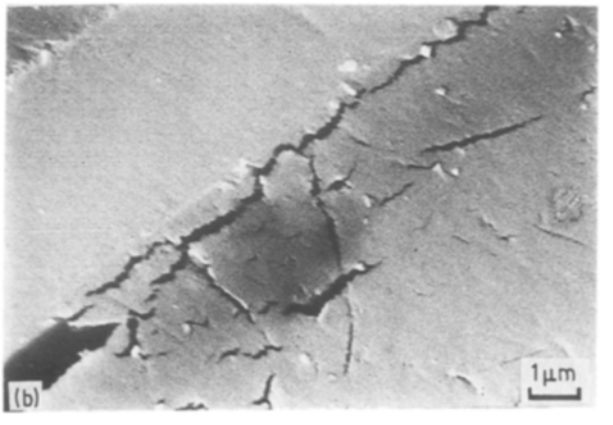

Figure 12 Slowly opened mode I crack in CF/epoxy (*in situ*).

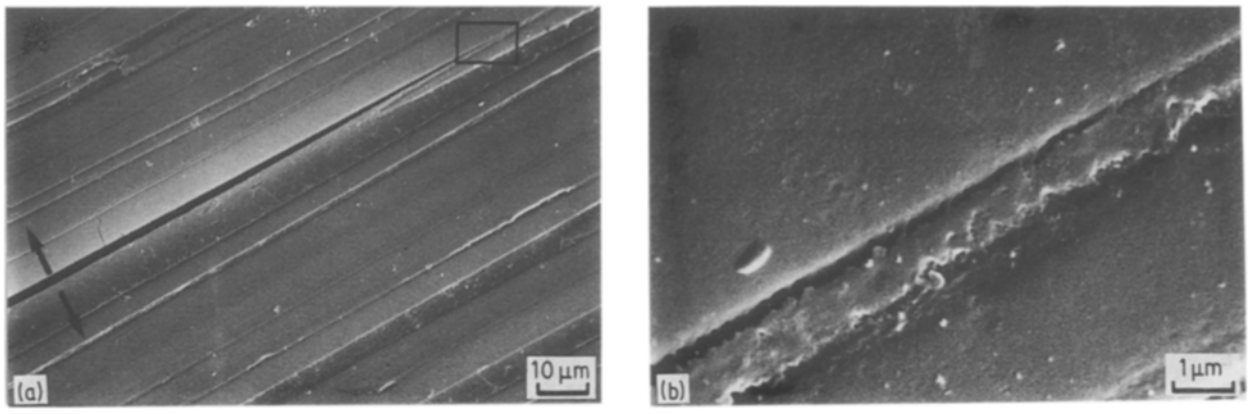

Figure 13 Fast propagated crack in CF/epoxy (mode I, *in situ*), showing (a) a smooth and sharp crack shape, and (b) no microcracking or damage in the polymer matrix ahead of the crack tip.

with different rates. The two mechanisms are the deformation imposed by the testing machine and the plastic zone development. When the rate of deformation imposed is greater than the rate of plastic zone development, the crack tip grows to the boundary of the plastic zone, and the crack tip sharpens until unstable growth occurs [14]. An alternative mechanism for stick–slip crack growth has been proposed by Kinloch *et al.* [7, 21, 22]. In their model the crack tip sticks due to blunting and slips because the time period during which the material can yield is reduced for the growing crack.

In mode II fracture, considerably less fibre bridging has been reported [3]. Wu [25], however, observed fibre bridging in pure mode II loading of glass/epoxy composites.

To study the extent of fibre bridging in the materials investigated as a function of mode of loading and deformation rate, the number of broken fibres per unit area of fracture surface was counted in the initiation and propagation regions of a crack increment. Fig. 17 exemplifies the counting of broken fibres on mode I and mode II fracture surfaces. The results of this counting procedure are listed in Table IV where the average number of broken fibres per mm^2 (average of three or more measurements) is given, along with the scatter. It is observed that an increase in crack tip displacement rate produces a somewhat larger number of broken fibres in the initiation region. This factor thus cannot explain the diminishing initiation toughness observed at high rates. Rather surprisingly mode II loading of CF/PEEK produces a larger number of broken fibres than mode I. The number of broken fibres in CF/PEEK fractured in mode I is generally larger in the propagation region than in the initiating region. This observation suggests, contrary to Berglund's proposed fibre-bridging mechanism for stick–slip behaviour [24], that the resistance to crack growth is larger in the region of unstable crack growth. If fibre bridging is responsible for stick–slip crack growth a smaller number of fractured fibres would be observed in the propagation region.

5. Conclusions

The previous sections outlined a model for micro-

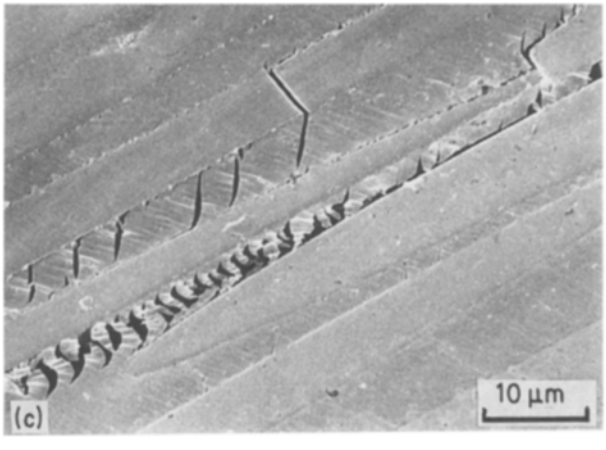

Figure 14 Higher magnifications of the damage zone ahead of a mode II crack in CF/PEEK: (a) 0.25 mm ahead; (b) 0.12 mm ahead; (c) 0.06 mm ahead.

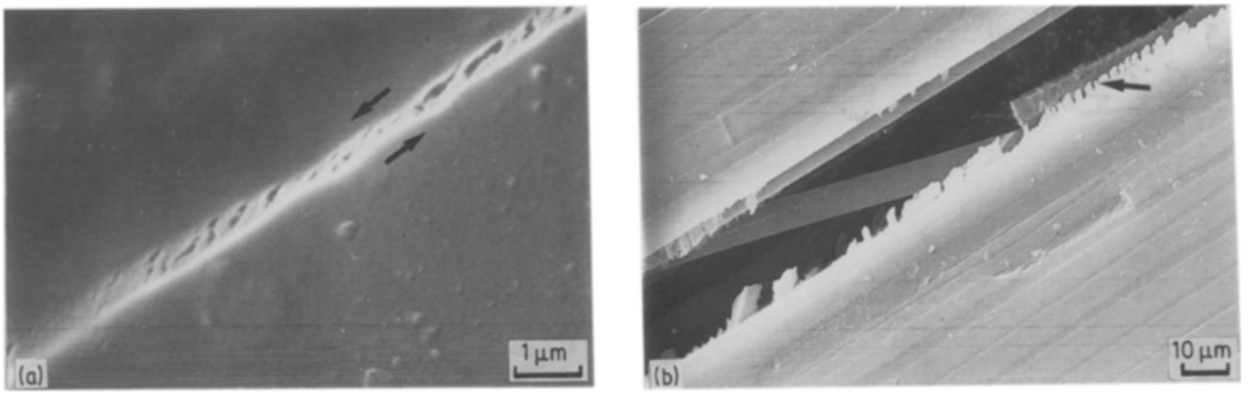

Figure 15 In situ mode II crack in CF/epoxy: (a) very high magnification of the region ahead of the crack tip; (b) crack with shear cusps as the edges (arrow) and a bridging fibre in the interior of the crack.

scopic mechanisms responsible for energy absorption during mode I and II fracture of unidirectional composites in the interlaminar plane. This model was used as a qualitative basis for an investigation of the underlying mechanisms for previously observed rate effects on mode I and II toughnesses. A quantitative comparison is not possible at this moment because many of the parameters in the model are yet undetermined.

Based on the results in this study the following conclusions can be drawn.

1. The rate dependency of composite toughness is similar to that of matrix toughness.

2. Limitations in toughness transfer from matrix to composite are most significant at low rates and are explained by restrictions imposed by the rigid fibres on the plastic zone size.

3. *In situ* SEM fracture studies provide experimental evidence of rate and matrix ductility on process zone size.

4. Fracture surface profiles partly explain rate effects in mode I interlaminar toughness, but do not explain rate effects observed in mode II.

5. Fibre bridging may increase the interlaminar toughness in mode I and mode II loading, but does not explain the observed rate effects or stick–slip growth observed in mode I fracture studies of PEEK matrix composites.

Acknowledgements

Thanks are due to the Center for Composite Materials (CCM) at the University of Delaware, and to the Department of Mechanical Engineering, Florida

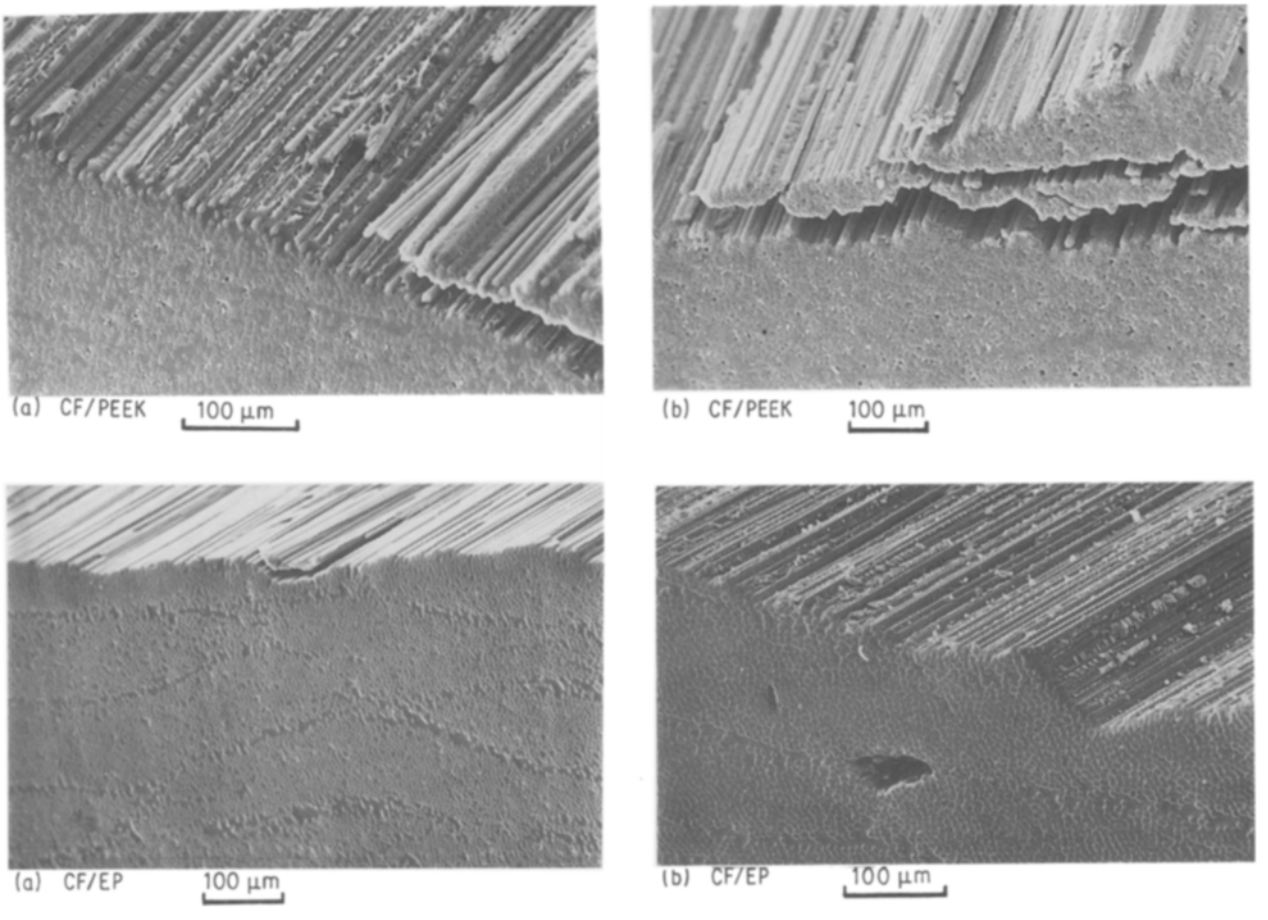

Figure 16 Examples of fracture surface profiles: (a) mode I; (b) mode II.

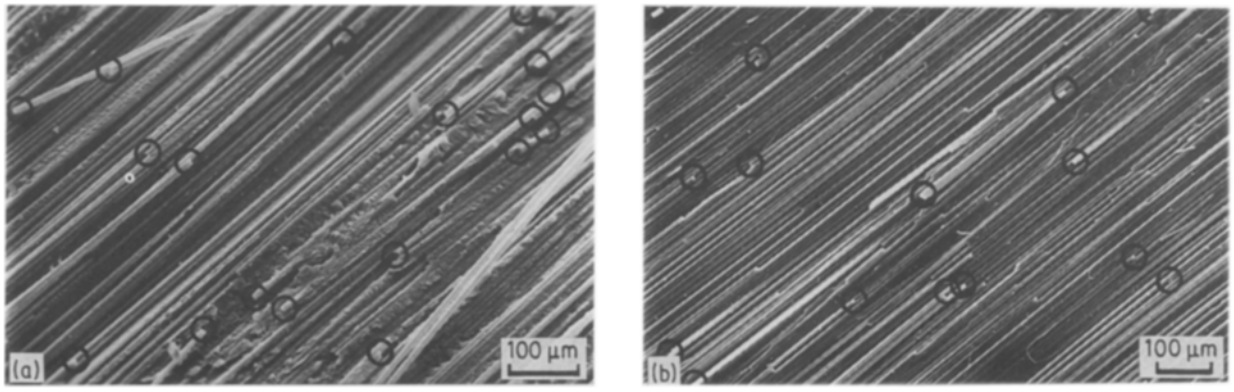

Figure 17 Examples of fibre breakages on fracture surfaces. (a) CF/PEEK, mode I (unstable propagation region), and (b) CF/epoxy, mode II (unstable propagation region).

TABLE IV Fibre fractures per unit area

Material	Mode	Crack tip displacement rate ($m\,sec^{-1}$)	Fibre fractures per mm^2	
			Initiation region	Propagation region
CF/PEEK	I	1×10^{-10}	35^{+8}_{-5}	62^{+28}_{-10}
CF/PEEK	I	4×10^{-6}	41^{+10}_{-8}	59^{+24}_{-38}
CF/epoxy	I	1×10^{-10}	43^{+2}_{-1}	38^{+2}_{-3}
CF/epoxy	I	1×10^{-6}	53^{+13}_{-20}	40^{+5}_{-8}
CF/PEEK	II	1×10^{-8}	49^{+10}_{-15}	80^{+9}_{-13}
CF/PEEK	II	7×10^{-6}	75^{+6}_{-11}	49^{+13}_{-20}
CF/epoxy	II	1×10^{-8}	21^{+11}_{-7}	30^{+8}_{-4}
CF/epoxy	II	5×10^{-6}	30^{+14}_{-13}	44^{+17}_{-18}

Atlantic University, for the support of this cooperative project. The authors appreciate the test materials donated by ICI and the help and cooperation of students and colleagues at the Technical University Hamburg-Harburg (TUHH) and CCM for their experimental and graphic designer works. The SEM studies at the TUHH were supported by the Deutsche Forschungsgemeinschaft (DFG-FRI 675-1-2).

References

1. D. J. WILKINS, "The Engineering Significance of Defects in Composite Structures", Conference Proceedings no. 355, Characterization, Analysis and Significance of Defects in Composite Materials organized by AGARD, 10–15 April 1983, London, UK.
2. D. L. HUNSTON, *Comp. Tech. Rev.* **4** (1986) 176.
3. A. J. RUSSELL and K. N. STREET, "Moisture and Temperature Effects on the Mixed Mode Delamination Fracture of Unidirectional Graphite/Epoxy", Delamination and Debonding of Materials, ASTM STP 876 (American Society for Testing and Materials, Philadelphia, Pennsylvania, USA, 1985) p. 349.
4. W. S. JOHNSON and P. D. MANGALGIRI, "Investigation of Fiber Bridging in Double Cantilever Beam Specimens", NASA TM 87716, April 1986.
5. W. L. BRADLEY and R. N. COHEN, "Matrix Deformation and Fracture in Graphite Reinforced Epoxies", Delamination and Debonding of Materials, ASTM STP 876 (American Society for Testing and Materials, Philadelphia, Pennsylvania, 1985) (American Society for Testing and Materials, Philadelphia, Pennsylvania) p. 389.
6. H. H. KAUSCH, "Polymer Fracture" (Springer Verlag, New York, 1978).
7. A. J. KINLOCH and R. J. YOUNG, "Fracture Behavior of Polymers" (Elsevier Applied Science, London, 1983).
8. J. G. WILLIAMS, "Fracture Mechanics of Polymers" (Ellis, Horwood Chichester, 1984).
9. K. FRIEDRICH, "Crazing in Shear Bands in Semi-Crystalline Polymers", in "Crazing in Polymers", edited by H. H. Kausch (Springer Verlag, New York, 1983).
10. A. J. SMILEY, M.S. Thesis, CCM-Report No. CCM-86-01, University of Delaware (1986).
11. A. J. SMILEY and R. B. PIPES, *J. Comp. Mater.* **21** (1987) 670.
12. *Idem*, *Comp. Sci. Tech.* **29** (1987) 1.
13. L. A. CARLSSON and R. B. PIPES, "Experimental Characterization of Advanced Composite Materials" (Prentice-Hall, New Jersey, 1987).
14. J. W. GILLESPIE Jr, L. A. CARLSSON and A. J. SMILEY, *Comp. Sci. Tech.* **28** (1987) 1.
15. L. A CARLSSON, J. W. GILLESPIE and B. R. TRETHEWEY, *J. Reinf. Plast. Comp.* **5** (1986) 170.
16. R. A. CRICK, D. C. LEACH, P. J. MEAKIN and D. R. MOORE, *J. Mater. Sci.* **22** (1987) 2094.

17. W. L. BRADLEY and W. M. JORDAN, "The Relationship between Resin Ductility and Composite Delamination Fracture Toughness", in Proceedings of International Symposium on Composite Materials and Structures, edited by T. T. Loo and C. T. Sun (Technomic, Lancaster, USA, 1986) p. 445.
18. R. W. LANG, M. HEYM, H. TESCH and H. STUTZ, "Influence of Constituent Properties on Interlaminar Crack Growth in Composites", in "High Tech – the Way into the Nineties", edited by K. Brunsch, H. D. Golden and C. M. Herkert (Elsevier, Amsterdam, 1986) p. 261.
19. K. FRIEDRICH, R. WALTER, H. VOSS and J. KARGER-KOCSIS, *Composites* **17** (1986) 205.
20. J. KARGER-KOCSIS and K. FRIEDRICH, *Plastics Rubber Proc. Appl.* **8** No. 2 (1987) 91–104.
21. A. J. KINLOCH, S. J. SHAW, D. A. TOD and D. L. HUNSTON, *Polymer* **24** (1983) 1341.
22. *Idem, ibid.* **24** (1983) 1355.
23. D. BROEK, "Elementary Engineering Fracture Mechanics," 3rd Edn (Martinus Nijhoff, 1984).
24. L. BERGLUND, PhD thesis no. 54, Linkoping University, Sweden (1985).
25. E. M. WU, "Strength and Fracture of Composites, Composite Materials", Vol. 5 "Fracture and Fatigue", edited by L. J. Broutman (Academic, New York, 1974) p. 191.

Received 1 July
and accepted 18 November 1988